Quantum computation using quantum dots

Xin Wang
City University of Hong Kong
(Dated: July 4, 2019)

I. OVERVIEW

Quantum computation has recently become an active field due to its potential to realize the next-generation computer granting us the ability to speed up exponentially without using an intractably large amount of physical resources. Feynman[1] proposed the first basic idea of the quantum computer, who realized that it is possible to simulate quantum systems using the quantum computer whose operations obey quantum mechanics. However, at that time, it is not completely clear to Feynman how one can realize such a quantum machine. After that, Divincenzo[2] proposed the general requirements for the quantum computer, what we now call the "Divincenzo criteria". In order to realize a quantum computer, we should have

- A scalable physical system with well characterized qubits.
- The ability to initialize the state of the qubits to a simple fiducial state.
- Long relevant decoherence times.
- A "universal" set of quantum gates.
- A qubit-specific measurement capability.
- The ability to interconvert stationary and flying qubits.
- The ability to faithfully transmit flying qubits between specified locations.

In order to construct the universal quantum computer, any potential candidate should safisfy the requirements above. A variety of physical systems are being developed over the past several decades including Nuclear Magnetic Resonance (NMR)[3], NV center[4], superconductor[5] and semiconductor quantum dot[6]. Each of the candidate has its own pros and cons to implement the physical operation. Among various issues, a common key problem is the decoherence. Decoherence comes from the noisy environment which will interact with the quantum system thus leading to loss of the quantum information carried and reducing the accuracy of the operation. To combat decoherence, various schemes[7–9] are proposed by researchers, among which the dynamically corrected gates (DCGs)[9–12] are useful measures, and there have been many proposals for spin qubits based on the semiconductor quantum-dot system in the literatures.

II. THE QUBIT

A classical bit can either be 0 or 1. A qubit can be in a linear superposition of two basis states $|0\rangle$ and $|1\rangle$ as

$$|\psi\rangle = \alpha|0\rangle + \beta|1\rangle, \tag{1}$$

where α and β are complex numbers, $|\alpha|^2 + |\beta|^2 = 1$, and states $|0\rangle$ and $|1\rangle$ are referred to as computational basis states. According to quantum mechanics, when we measure such a qubit state, we may either get the result $|0\rangle$ with probability $|\alpha|^2$, or result $|1\rangle$ with probability $|\beta|^2$.

On the other hand, $|\psi\rangle$ can be regarded as a unit vector in a two-dimensional Hilbert space as

$$|\psi\rangle = \begin{pmatrix} \alpha \\ \beta \end{pmatrix}. \tag{2}$$

A quantum gate is an operation on the qubit. It can be represented by a matrix. A single-qubit gate can be represented as a 2×2 matrix. For example, the NOT gate is

$$X \equiv \begin{pmatrix} 0 & 1 \\ 1 & 0 \end{pmatrix}, \tag{3}$$

which essentially to flips the qubit:

$$X \begin{pmatrix} \alpha \\ \beta \end{pmatrix} = \begin{pmatrix} \beta \\ \alpha \end{pmatrix}. \tag{4}$$

It is named X because it is identical to the Pauli X matrix. As we will see later, Pauli matrices play a key role in representing quantum gates.

Note that any quantum gate U must be unitary, i.e. $UU^\dagger = I$. One can easily verify that $XX^\dagger = I$. Another example is the Z gate:

$$Z \equiv \begin{pmatrix} 1 & 0 \\ 0 & -1 \end{pmatrix}, \tag{5}$$

which changes $|1\rangle$ to $-|1\rangle$ (we say it adds a "phase factor" to the state) and leaves $|0\rangle$ unchanged. The Z gate corresponds to the Pauli Z matrix, and we can similarly define the Y gate, and more generally, $\exp\{-i(\hat{\sigma}\cdot\hat{r})\phi/2\}$.

The Hadamard gate is also frequently used. It acts like a "square-root of NOT" gate and turns the state $|0\rangle$ into $(|0\rangle + |1\rangle)/\sqrt{2}$ and $|1\rangle$ into $(|0\rangle - |1\rangle)/\sqrt{2}$:

$$H \equiv \frac{1}{\sqrt{2}} \begin{pmatrix} 1 & 1 \\ 1 & -1 \end{pmatrix}. \tag{6}$$

There are infinitely many single-qubit gates. It turns out that an arbitrary 2×2 unitary single-qubit gate can be decomposed as[13]

$$U = e^{i\alpha} \begin{pmatrix} e^{-i\beta/2} & 0 \\ 0 & e^{i\beta/2} \end{pmatrix} \begin{pmatrix} \cos\frac{\gamma}{2} & -\sin\frac{\gamma}{2} \\ \sin\frac{\gamma}{2} & \cos\frac{\gamma}{2} \end{pmatrix} \begin{pmatrix} e^{-i\delta/2} & 0 \\ 0 & e^{i\delta/2} \end{pmatrix}. \tag{7}$$

A qubit can alternatively be described geometrically. We rewrite Eq. (1) as

$$|\psi\rangle = \cos\frac{\theta}{2}|0\rangle + e^{i\phi}\sin\frac{\theta}{2}|1\rangle, \tag{8}$$

where θ and ϕ are real numbers which correspond to the angular component of the spherical coordinates. A pair of θ and ϕ therefore uniquely define a point on the surface of a sphere, called the *Bloch sphere* (cf. Fig. 1). Exception: $\theta = 0$ or π refers to the north or south pole respectively, regardless of the value of ϕ.

With the geometrical representation, we can rephrase the single-qubit gates as "rotations". To see why, let us consider a gate defined as

$$R(\hat{z}, \phi) = \exp\{-i\sigma_z\phi/2\}. \tag{9}$$

Note that

$$\begin{aligned} R(\hat{z},\phi)|\psi_0\rangle &= \exp\{-i\sigma_z\phi/2\} \cdot \begin{pmatrix} \cos\frac{\theta_0}{2} \\ e^{i\phi_0}\sin\frac{\theta_0}{2} \end{pmatrix} \\ &= \begin{pmatrix} e^{-i\phi/2} & 0 \\ 0 & e^{i\phi/2} \end{pmatrix} \cdot \begin{pmatrix} \cos\frac{\theta_0}{2} \\ e^{i\phi_0}\sin\frac{\theta_0}{2} \end{pmatrix} \\ &= e^{-i\phi/2} \begin{pmatrix} \cos\frac{\theta_0}{2} \\ e^{i(\phi_0+\phi)}\sin\frac{\theta_0}{2} \end{pmatrix} \end{aligned} \tag{10}$$

so it acts like rotating the Bloch vector around the z axis by an additional angle ϕ.

One can also view this from a slightly different angle. Suppose one has a system described by the Hamiltonian (which is actually a magnetic field along the z direction with strength/amplitude h)

$$H = h\sigma_z. \tag{11}$$

The Hamiltonian has two eigenstates $|0\rangle$ (with eigenenergy $E_0 = h$) and $|1\rangle$ (with eigenenergy $E_0 = -h$). Suppose the qubit is initialized as

$$|\psi_0\rangle = \alpha_0|0\rangle + \beta_0|1\rangle \tag{12}$$

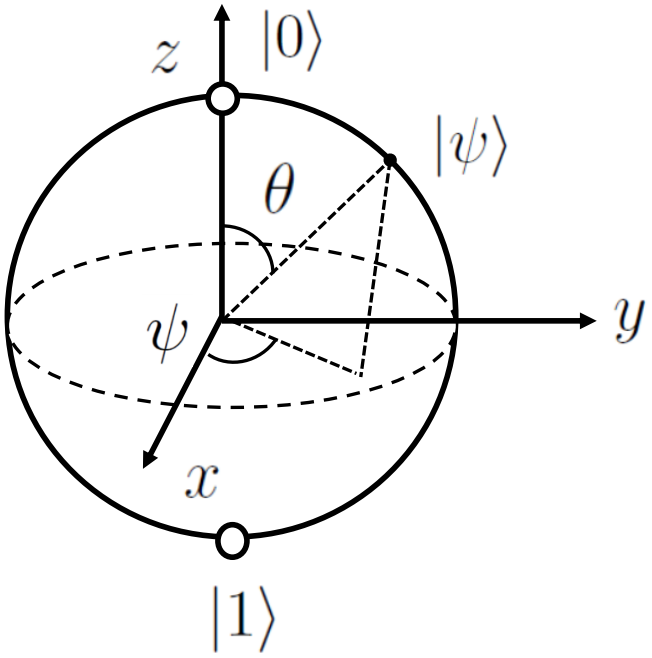

FIG. 1: A qubit represented on the Bloch sphere.

Under the evolution of H, the two components of the qubit will acquire different phases:

$$\begin{aligned} |\psi(t)\rangle &= e^{-iHt}|\psi_0\rangle \\ &= \alpha_0 e^{-iht}|0\rangle + \beta_0 e^{iht}|1\rangle \\ &= e^{-iht}\left(\alpha_0|0\rangle + \beta_0 e^{2iht}|1\rangle\right) \end{aligned} \tag{13}$$

So that if one holds the magnetic field at h for a time t, the rotation it incurs is

$$e^{-iHt} = e^{-ih\sigma_z t} = e^{-i\sigma_z \frac{2ht}{2}} \tag{14}$$

which rotates the Bloch vector around the z axis by an angle $2ht$.

This understanding is essential to quantum control of spin qubits.

One can similarly prove that a rotation around an arbitrary axis $\hat{r}$ can be represented by

$$R(\hat{r}, \phi) = \exp\{-i(\hat{\sigma} \cdot \hat{r})\phi/2\}. \tag{15}$$

For two qubits, there are four computational basis states $|00\rangle$, $|01\rangle$, $|10\rangle$, and $|11\rangle$. A two-qubit state can be described as

$$|\psi\rangle = \alpha|00\rangle + \beta|01\rangle + \gamma|10\rangle + \delta|11\rangle, \tag{16}$$

where α, β, γ and δ are complex numbers, $|\alpha|^2 + |\beta|^2 + |\gamma|^2 + |\delta|^2 = 1$. Also we can use a vector to describe such a two qubit state denoted as

$$\begin{pmatrix} \alpha \\ \beta \\ \gamma \\ \delta \end{pmatrix}, \tag{17}$$

and two-qubit gates are 4×4 matrices.

The most important two-qubit gate is the *controlled*-NOT gate (CNOT) A CNOT gate can be described by a 4×4 matrix as

$$\text{CNOT} = \begin{pmatrix} 1 & 0 & 0 & 0 \\ 0 & 1 & 0 & 0 \\ 0 & 0 & 0 & 1 \\ 0 & 0 & 1 & 0 \end{pmatrix}. \tag{18}$$

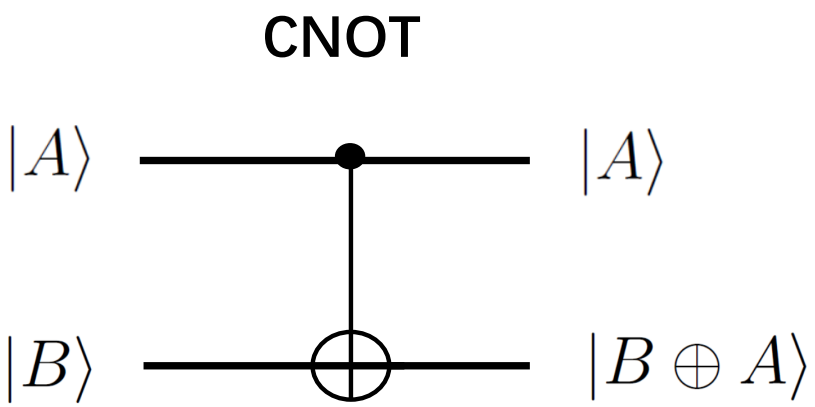

FIG. 2: Quantum circuit of a CNOT gate.

The CNOT gate acts on the two-qubit states where the first qubit is the control qubit and the second the target. After the CNOT operation, if the control qubit is $|0\rangle$, then the target qubit keeps unchanged. However, if the control qubit is "set", i.e. $|1\rangle$, the CNOT gate flips the target qubit. Such action can be summarized as $|A, B\rangle \rightarrow |A, B \oplus A\rangle$.

It turns out that arbitrary single-qubit operation plus one entangling two-qubit operation suffices for universal quantum computation.[13]

III. SPIN QUBITS

Among various candidates for the physical realization of a quantum computer, semiconductor quantum-dot systems stand out due to the long coherence time[14], the advantage of implementing the fast all-electrical gate operations[15] and most importantly the prospective scalability[16]. Semiconductor quantum dots are artificial systems which are fabricated based on semiconductor substrates. GaAs is the first demonstrated material for fabricating quantum dots to perform spin qubit operations due to its high mobility of electrons[15]. Fig. 3 shows a diagram of a GaAs-based quantum-dot system. As illustrated, the system is a two-dimensional structured surface consisting of some electrodes (which control the qubit via gate voltages) and sensors. The electrodes on the surface can help to form the potential well to confine electrons below the surface. The number of the electrons and the inter-dot tunnel coupling between the left and the right dot can be adjusted by applying voltage pulses. On the other hand, the readout procedure can be implemented by the sensitive quantum point contact (QPC) sensor which is next to one of the quantum dots. When an electron is transferred from one dot to the other, the conductance gives a distinct value corresponding to the charge state.

The original idea of spin qubit using quantum dot is from[6], where a single electron spin was encoded as a qubit (LD qubit). Inspired by the initial idea of Loss and DiVincenzo, many proposals have been put forward. Fig. 4 shows various types of spin qubits for different semiconductor quantum-dot systems, each of which is described by the charge stability and the energy spectrum. The left column of Fig. 4 shows the charge occupancy for each spin qubit which is tuned by the gate voltages V_L and V_R. As we can see that apart from the LD qubit encoding a qubit with a single electron spin, other proposals require two or more electrons. The right column of Fig. 4 shows the energy spectra. The energy for each qubit except for LD qubit is as a function of the detuning ϵ which is the potential difference between the related dots and can be tuned easily by the gate voltage. And we also can see that each spin qubit is working in different charge regime. Next, we would describe each of the spin qubit in datail.

IV. LOSS-DIVINCENZO QUBIT

LD qubit is the first demonstrated spin qubit proposed by[6] based on a semiconductor quantum dot. As mentioned above, LD qubit works with a single electron spin in a single quantum dot. The computational basis states are the different spin states, namely, spin up and down. As seen in Fig. 4, the energy levels of the spin states are adjusted by tuning the static magnetic field B_0. The energy splitting becomes larger when B_0 is increased. The splitting Zeeman energy is $E_z = g\mu_B B_0$ where g is the electron g-factor and μ the Bohr magneton. The effective Hamiltonian in terms

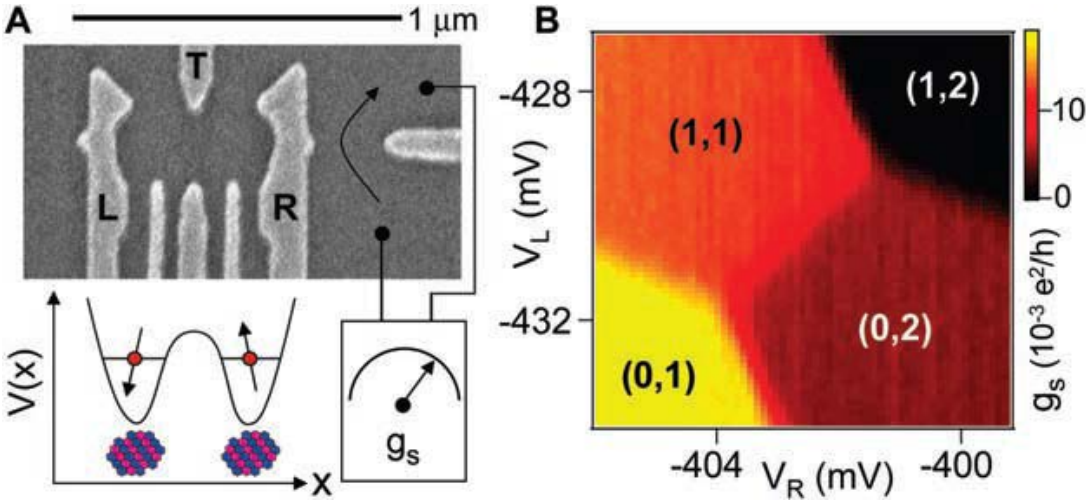

FIG. 3: Schematic of the semiconductor quantum-dot system based on GaAs heterostructure[15].

of the Pauli operators can be written as

$$H_0 = \frac{g\mu_B B_0}{2}\sigma_z = \omega_0 S_z, \tag{19}$$

where ω_0 is the Larmor angular frequency and $S_z = \sigma_z/2$ (theoreticians always take $\hbar = 1$) is the spin operator.

The full single-qubit operation of LD qubit is done in the rotating frame. Consider the full Hamiltonian,

$$\begin{aligned} H_0 &= \omega_0 S_z, \\ H_1 &= JS_x = \left[J_1 + J_2\cos(\omega t + \varphi)\right] S_x. \end{aligned} \tag{20}$$

In the rotating frame of H_0, we have,

$$\begin{aligned} H_{\text{eff}} &= \boldsymbol{e}^{\boldsymbol{i}H_0 t} H_1 \boldsymbol{e}^{-\boldsymbol{i}H_0 t} \\ &= \boldsymbol{e}^{\frac{i\omega_0 t\sigma_z}{2}} \frac{J}{2}\sigma_x \boldsymbol{e}^{\frac{-i\omega_0 t\sigma_z}{2}} \\ &= \begin{bmatrix} \boldsymbol{e}^{\frac{i\omega_0 t}{2}} & 0 \\ 0 & \boldsymbol{e}^{-\frac{i\omega_0 t}{2}} \end{bmatrix} \begin{bmatrix} 0 & \frac{J}{2} \\ \frac{J}{2} & 0 \end{bmatrix} \begin{bmatrix} \boldsymbol{e}^{-\frac{i\omega_0 t}{2}} & 0 \\ 0 & \boldsymbol{e}^{\frac{i\omega_0 t}{2}} \end{bmatrix} \\ &= \begin{bmatrix} 0 & \frac{J}{2}\boldsymbol{e}^{i\omega_0 t} \\ \frac{J}{2}\boldsymbol{e}^{-i\omega_0 t} & 0 \end{bmatrix} \end{aligned} \tag{21}$$

For the element $\frac{J}{2}\boldsymbol{e}^{-\boldsymbol{i}\omega_0 t}$,

$$\begin{aligned} \frac{J}{2}\boldsymbol{e}^{-\boldsymbol{i}\omega_0 t} &= \frac{1}{2}\left[J_1 + J_2\cos(\omega t + \varphi)\right]\boldsymbol{e}^{-\boldsymbol{i}\omega_0 t} \\ &= \frac{1}{2}\left[J_1 + \frac{1}{2}J_2\boldsymbol{e}^{\boldsymbol{i}(\omega t+\varphi)} + \frac{1}{2}J_2\boldsymbol{e}^{-\boldsymbol{i}(\omega t+\varphi)}\right]\boldsymbol{e}^{-\boldsymbol{i}\omega_0 t} \\ &= \frac{1}{2}J_1\boldsymbol{e}^{-\boldsymbol{i}\omega_0 t} + \frac{1}{4}J_2\boldsymbol{e}^{\boldsymbol{i}[(\omega-\omega_0)t+\varphi]} + \frac{1}{4}J_2\boldsymbol{e}^{-\boldsymbol{i}[(\omega+\omega_0)t+\varphi]} \end{aligned} \tag{22}$$

Up to this point it is still exact. Now we are going to make the famous Rotating Wave Approximation (RWA). The idea is that if a term is oscillating fast enough, it is going to average (close) to zero if the evolution is long enough. Therefore the only term that is important is the one involving $\omega - \omega_0$ as that becomes zero when $\omega = \omega_0$ (a condition we call "on resonance"). If it is not oscillating at all, it is not going to average to zero. Both other terms average close to zero.

When ω_0 is large enough, and $\omega \sim \omega_0$, Eqs. 22 becomes

$$\frac{J}{2}\boldsymbol{e}^{-\boldsymbol{i}\omega_0 t} \approx \frac{1}{4}J_2\boldsymbol{e}^{\boldsymbol{i}[(\omega-\omega_0)t+\varphi]}\Big|_{\omega=\omega_0} = \frac{J_2}{4}\boldsymbol{e}^{\boldsymbol{i}\varphi} \tag{23}$$

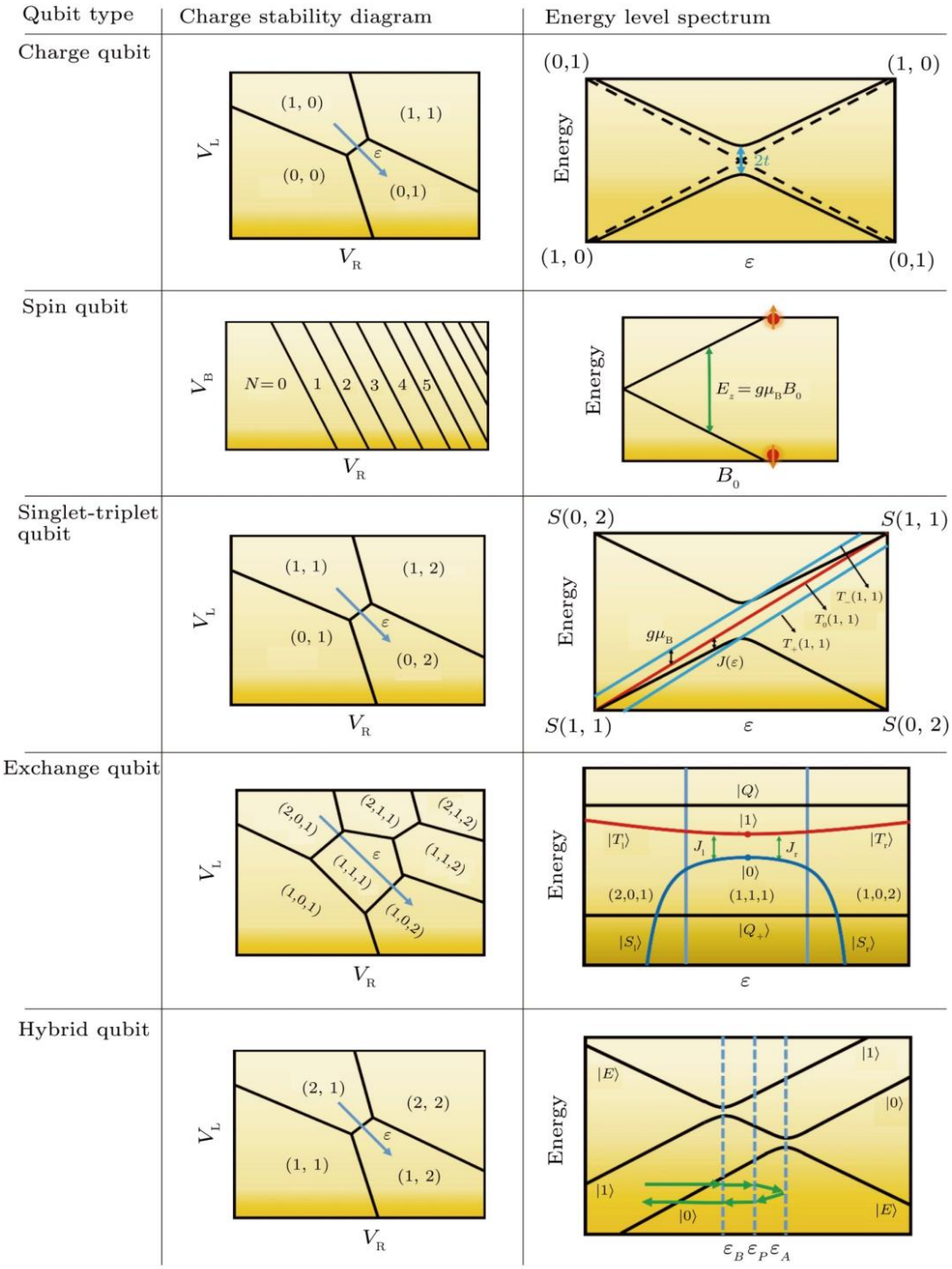

FIG. 4: Spin qubits for semiconductor quantum-dot systems[17]. The left column represents the charge occupancy for each proposal and the right column the corresponding energy spectrum. Note that in this thesis we only focus on spin qubits.

This approximation is RWA. Then the effective Hamiltonian Eqs. 21 can be written as,

$$\begin{aligned} H_{\text{eff}} &= \begin{bmatrix} 0 & \frac{J_2}{4}\boldsymbol{e}^{-\boldsymbol{i}\varphi} \\ \frac{J_2}{4}\boldsymbol{e}^{\boldsymbol{i}\varphi} & 0 \end{bmatrix} \\ &= \begin{bmatrix} 0 & \frac{J_2}{4}\cos\varphi - \frac{J_2}{4}\boldsymbol{i}\sin\varphi \\ \frac{J_2}{4}\cos\varphi + \frac{J_2}{4}\boldsymbol{i}\sin\varphi & 0 \end{bmatrix} \\ &= \frac{J_2}{4}\left(\cos\varphi\sigma_x + \sin\varphi\sigma_y\right) \\ &= \frac{J_2}{4}\left(\cos\varphi, \sin\varphi, 0\right)\cdot\boldsymbol{\sigma} \end{aligned} \tag{24}$$

So as we control the phase of the microwave, we control the rotating axis. The amplitude of the microwave gives the rotating rate.

Here are some points worth to remember:

1. The condition of RWA is (a) $\omega, \omega_0 \gg 0$ and (b) $\omega \sim \omega_0$;
2. Under RWA J_1 does nothing to the rotation;
3. J_2 corresponds to the control strength. The angle of rotation is $\theta = \frac{J_2}{4}t\cdot 2 = \frac{J_2 t}{2}$ and the angular velocity is $\frac{J_2}{2}$;
4. The rotation axis can be adjusted by the microwave phase φ: $(\cos\varphi, \sin\varphi, 0)$,
   (a) when $\varphi = 0$, the rotation axis is $x-$axis;
   (b) when $\varphi = \frac{\pi}{2}$, the rotation axis is $y-$axis.

The two-qubit gate for LD qubit is performed using the Heisenberg exchange interaction. One can check the original paper by Loss and Divincenzo.[6]

---

[1] R. P. Feynman, International journal of theoretical physics **21**, 467 (1982), URL `https://link.springer.com/article/10.1007%2FBF02650179`.
[2] D. P. DiVincenzo et al., arXiv preprint quant-ph/0002077 (2000).
[3] L. M. Vandersypen, M. Steffen, G. Breyta, C. S. Yannoni, M. H. Sherwood, and I. L. Chuang, Nature **414**, 883 (2001).
[4] M. G. Dutt, L. Childress, L. Jiang, E. Togan, J. Maze, F. Jelezko, A. Zibrov, P. Hemmer, and M. Lukin, Science **316**, 1312 (2007).
[5] J. Clarke and F. K. Wilhelm, Nature **453**, 1031 (2008).
[6] D. Loss and D. P. DiVincenzo, Phys. Rev. A **57**, 120 (1998).
[7] S.-L. Zhu, Z. Wang, and P. Zanardi, Phys. Rev. Lett. **94**, 100502 (2005).
[8] X. Chen, I. Lizuain, A. Ruschhaupt, D. Guéry-Odelin, and J. G. Muga, Phys. Rev. Lett. **105**, 123003 (2010), URL `https://link.aps.org/doi/10.1103/PhysRevLett.105.123003`.
[9] X. Wang, L. S. Bishop, J. P. Kestner, E. Barnes, K. Sun, and S. Das Sarma, Nature Commun. **3**, 997 (2012).
[10] G. T. Hickman, X. Wang, J. P. Kestner, and S. Das Sarma, Phys. Rev. B **88**, 161303 (2013).
[11] X. Wang, L. S. Bishop, E. Barnes, J. P. Kestner, and S. Das Sarma, Phys. Rev. A **89**, 022310 (2014).
[12] C. Zhang, X.-C. Yang, and X. Wang, Phys. Rev. A **94**, 042323 (2016), URL `https://link.aps.org/doi/10.1103/PhysRevA.94.042323`.
[13] M. A. Nielsen and I. L. Chuang, *Quantum computation and quantum information* (Cambridge University Press, Cambridge, 2010).
[14] H. Bluhm, S. Foletti, I. Neder, M. Rudner, D. Mahalu, V. Umansky, and A. Yacoby, Nat. Phys. **7**, 109 (2011).
[15] J. Petta, A. Johnson, J. Taylor, E. Laird, A. Yacoby, M. Lukin, C. Marcus, M. Hanson, and A. Gossard, Science **309**, 2180 (2005).
[16] J. Taylor, H. Engel, W. Dur, A. Yacoby, C. Marcus, P. Zoller, and M. Lukin, Nature Phys. **1**, 177 (2005).
[17] X. Zhang, H.-O. Li, K. Wang, G. Cao, M. Xiao, and G.-P. Guo, Chin. Phys. B **27**, 020305 (2018).